Nonadiabatic Dynamics of the Electromagnetic Field and Charge Carriers in High-Q Photonic Crystal Resonators

A. M. Yacomotti,* F. Raineri, C. Cojocaru, P. Monnier, J. A. Levenson, and R. Raj

Laboratoire de Photonique et de Nanostructures (CNRS UPR 20), Route de Nozay - 91460 Marcoussis-France

(Received 7 June 2005; published 9 March 2006)

We address, both experimentally and theoretically, phase and amplitude dynamics of the electromagnetic field in a two-dimensional photonic crystal when femtosecond pulses are injected. We demonstrate that the usual adiabatic approximation underlying the dynamics of field and carriers in a semiconductor resonator is no longer valid, since in general the photon lifetime cannot be neglected with respect to the carrier recombination lifetime. Parameter regions where adiabaticity is broken are shown, and the ubiquity of the observed dynamical scenario in the new generation of active photonic microresonators is predicted.

DOI: 10.1103/PhysRevLett.96.093901 PACS numbers: 42.70.Qs, 42.60.Da, 42.65.Sf

One of the most interesting features of photonic crystals (PCs) is their versatility to host microresonators with extremely high quality (high-Q) factors [1]. This, combined with active materials, for instance, semiconductors, opens innovative ways to control light [enhancing light-matter interaction [2], stopping and storage of light [3], quantum information processing [4], etc.] leading to a large variety of applications towards fully integrated optical devices [5–7].

In such active resonators, the electromagnetic field dynamics depends on two time scales. The first one is the time scale for the electromagnetic field development in the cavity (τ_E) that ranges from few (in our two-dimensional —2D— PC) to several tens of picoseconds [in recent 2DPC microcavities [1]] in high-Q systems. The second one is the material response time, i.e., the electron-hole recombination time (τ_r) in the semiconductor. In 2DPC, τ_r is strongly reduced mainly due to nonradiative recombination at the semiconductor/air etched interfaces. The ratio between these two time scales dramatically influences the dynamics. For well-known semiconductor microcavities such as vertical cavity surface emitting lasers, τ_E remains typically 3 orders of magnitude below τ_r; under short optical excitations, this results in a dynamical response which is characterized as the carriers being ''frozen'' during τ_E, known as the adiabatic regime. In contrast, in current PCs, τ_E gets closer and closer to τ_r, meaning that the field time scale is no longer negligible with respect to the carrier time scale. Fast carrier dynamics is then expected to modify the phase and amplitude of the electromagnetic field.

In this Letter we show, using femtosecond pump and probe experiments, that the dynamics of light-matter interaction in photonic crystal microresonators is governed by a subtle interplay between the carrier dynamics and the traveling photons in the early stages after the pumping pulse arrival. This breaks down the adiabatic regime that typically holds in other standard semiconductor microcavities.

Let us represent an ideal situation where the optical electrical field $\mathcal{E} = \mathrm{Re}[E(t)\exp(-i\omega_c t)]$ in a resonator, where E is the amplitude and ω_c the central frequency of the resonance (the reference frequency), is turned on by a short probe pulse. The latter is short enough to be considered as an optical kick excitation. The field-amplitude relaxation is much slower, considered exponential, with decay time equal to $2\tau_p$ (see Fig. 1). As the pump arrives, for example, after the probe, a carrier population is created, also in an instantaneous fashion. Now the cavity resonance is shifted since the refraction index has changed, becoming detuned with respect to ω_c [8]. As a result, $\mathrm{Re}\,(E)$ oscillates. In addition, the frequency of the oscillation varies because of carriers relaxation. Our goal is to show that this simple picture can capture the essence of the dynamical processes in active 2DPCs under short-pulse excitation.

The experiments were carried out in a 2D PC 237 nm-thick InP slab with a graphite lattice of air holes [lattice constant = 770 nm, see [8] for details], incorpo-

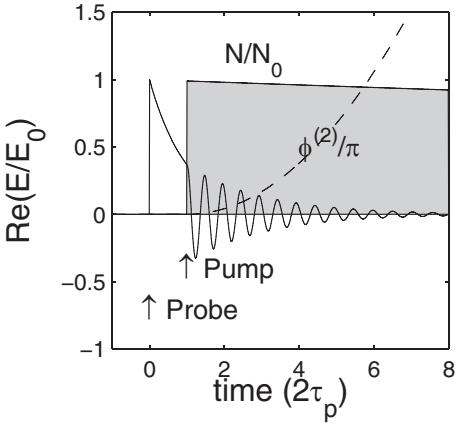

FIG. 1. Electric field (solid line), second order phase (dashed line), and carriers dynamics (solid line with shadow) for typical pump and probe delay. The shadow represents that the medium is active. Traces correspond to Eqs. (3) and (4) with $N_0 = 0.5$ and $\gamma = 0.02$.

rating four quantum wells emitting at 1450 nm. The 2DPC was designed in order to exhibit a flat photonic band edge at the Γ point (normal incidence) around 1540 nm, which is largely detuned from maximum of absorption. The consequently low group velocity mode behaves as high-Q 2D "in-plane resonator," confining the photons in the slab. The resulting optical resonance has a FWHM of 0.54 nm, giving a quality factor of $Q = 2860$ and photon lifetime of $\tau_p = 2.3$ ps.

The sample is explored via time-resolved pump and probe spectroscopy using 120 fs pulses at 810 nm for the pump, and around 1550 nm for the probe. Both beams are normally incident and spatially overlapped onto the sample. They are focused down through an achromatic microscope objective to spot diameters of 10 μm and 5 μm for pump and probe, respectively. The probe is linearly polarized in the ΓK direction of the reciprocal lattice, which was found to optimize the coupling of the probe field into the resonance. The spectral width of the probe pulses is 25 nm allowing to obtain a complete spectrum without varying the central wavelength. The pumping pulse is mainly absorbed in the quantum barriers, i.e., incoherently with respect to electron-hole recombination transitions or photonic resonances. The relative delay between pump and probe pulses is defined as $t_0 = \Delta t/2\tau_p = (t_{\text{pump}} - t_{\text{probe}})/2\tau_p$.

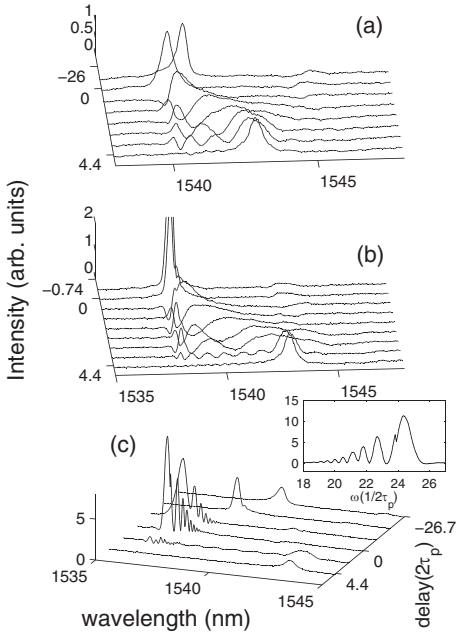

FIG. 2. Experimental optical spectra. Pumping levels are $N_0 = 0.3$ in (a), 0.6 in (b), and 0.9 in (c). Each curve corresponds to a pump-probe delay; positive delays mean pump arriving after the probe. Normalized delays are: (a) $t_0 = 4.4, 1.8, 1.36, 0.78, 0.56, 0.19, -0.67, -26$; (b) $t_0 = 4.4, 2.17, 0.78, 0.63, 0.4, 0.28, 0.06, -0.3, -0.74$; (c) $t_0 = 4.4, 2.1, -0.09$ (also in the inset), $-0.15, -11.5, -26.7$ from the front curve to the back curve.

In Fig. 2 we show optical spectra of the probe reflection on the sample for three pumping levels: 0.4, 0.8, and 1.3 mW, corresponding to $N_0 = 0.3$, 0.6, and 0.9 respectively (N_0 is pumping intensity normalized to laser intensity threshold, $\langle I_{p,\text{th}}\rangle = 4.58$ kW/cm^2). Several pump-probe delays are set for each pumping level; curves in the front ($t_0 > 0$) correspond to probe pulse anticipating pump pulse, while curves in the back ($t_0 < 0$) correspond to pump pulse anticipating probe pulse.

Two kinds of spectral oscillations can be distinguished: we call "type 1" oscillations those of Figs. 2(a) and 2(b) occurring for pump arriving after the probe pulse ($t_0 > 0$). Their spectral period changes with the delay, becoming shorter for large t_0. The second type of oscillations, that we call "type 2," are fast oscillations and occur close to the laser threshold around $t_0 = 0$ [Fig. 2(c), see inset for the curve $t_0 = -0.09$ alone].

The main approximation in our theoretical approach is to associate the observed resonance with a longitudinal mode of a Fabry-Perot-like resonator filled with a semiconductor medium, which allows us to dramatically simplify the description. The model can be derived from the Maxwell-Bloch equations, in the rotating wave and slowly varying approximations with adiabatic elimination of the polarization, and finally performing the mean field limit. The first two ones are standard approximations in many problems of nonlinear optics, and the latter is justified since: (i) the system is single mode, i.e., only one photonic mode is present inside the injection pulse spectrum [9], and (ii) the cavity has a large Q factor. The equations for the electric field amplitude E and the carriers population N read, in their adimensional form [10],

$$\frac{\partial E}{\partial t} = -E - (i\alpha - 1)NE \tag{1}$$

$$\frac{\partial N}{\partial t} = -\gamma[N + (N - N_t)|E|^2], \tag{2}$$

with initial conditions $E(t = 0) \equiv E_0 \propto \sqrt{\langle I_I\rangle/I_{\text{sat}}}$ and $N(t = t_0) \equiv N_0 = \langle I_p\rangle/\langle I_{p,\text{th}}\rangle$, where I_I is the injection (probe) intensity and I_{sat} is the saturation intensity. Note that both pumping and probing are approximated to give kicklike responses in carriers and field, respectively, due to the fact that the input pulse duration is much shorter than both the carriers relaxation time (τ_r) and photon lifetime. Normalizations are such that $|E|^2 = I/I_{\text{sat}}$, where I is the circulating intensity in the resonator; N is carriers density normalized to that at laser threshold; time is normalized to $2\tau_p$. The parameter α is the ratio between the real and the imaginary parts of the differential susceptibility at the central frequency of the optical resonance [11]; $\gamma = 2\tau_p/\tau_r$; N_t is the normalized carriers density at transparency.

Let us first consider the pump pulse arriving at $t_0 = 0$; Eq. (1) can be straightforwardly integrated and gives $E(t) = E_0 \exp[-t + (1 - i\alpha)\int_0^t N(\tau)d\tau]$. As long as

$|E_0|^2 \ll 1$ and $N_0 \leq 1$, $\int_0^t N(\tau)d\tau$ can be approximated by $N_0(1 - \gamma t/2)t$ inside the exponential, since for small γ (here we consider $\gamma = 0.02$), it results $\gamma t \ll 1$ where $E(t)$ does not vanish.

The solution of (1) and (2) is thus $E(t) = A(t) \times \exp[i\phi(t)]$, with

$$A(t) \simeq E_0 \exp\left[-\frac{\gamma N_0}{2}\left(t + \frac{(1-N_0)}{N_0\gamma}\right)^2 + \frac{(1-N_0)^2}{2N_0\gamma}\right] \quad (3)$$

$$\phi(t) \simeq -\alpha N_0\left(1 - \frac{\gamma t}{2}\right)t. \quad (4)$$

We first define the adiabatic limit, valid when $|\phi^{(2)}(t)| = |d^2\phi/dt^2|t^2/2 \ll \pi$, then $t \ll \sqrt{2\pi/\alpha N_0\gamma} \equiv t_a$. The phase becomes $\phi(t) = \phi^{(1)}(t) = -\Omega t$, where $\Omega \equiv \alpha N_0$ is the pump-induced frequency shift. The decay time of the field amplitude δt_E for arbitrary $N_0 \leq 1$ can be easily derived from Eq. (3). The condition for the adiabatic regime to be valid becomes $\delta t_E \ll t_a$. The adiabatic condition is fully verified for $N_0 = 0.3$, and marginally for $N_0 = 0.6$. This is illustrated in Fig. 1: for $N_0 = 0.5$, $\phi^{(2)}/\pi < 1$ during the field decay, meaning that the adiabatic approximation is valid. In contrast, for values of $N_0 \gtrsim 0.8$, $\phi^{(2)}/\pi$ reaches unity *before* the field has fallen to $1/e$ of its maximum. "Type 1" oscillations observed in the experimental spectra are captured by the adiabatic limit when the pump arrives after the probe. The electric field dynamics for $t_0 \geq 0$ can be written in a compact form

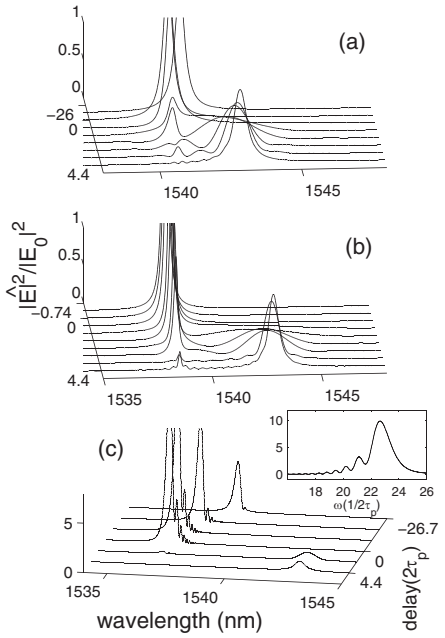

FIG. 3. Theoretical optical spectra. (a) $N_0 = 0.3$ and (b) $N_0 = 0.6$ are calculated from Eq. (6); (c) $N_0 = 0.9$ is the power spectrum of Eq. (5) with (3) and (4). Normalized delays are the same as the experimental ones. Inset: $t_0 = 0$.

$$E(t;t_0) = \theta(t)\theta(t_0 - t)E_0\exp(-t) + \theta(t - t_0)A(t - t_0)\exp[-t_0 + i\phi(t - t_0)], \quad (5)$$

where $\theta(t)$ is the Heaviside function. For $N_0 = 0.3$ the adiabatic limit yields $\phi = \phi^{(1)}$ and $A(t) = E_0\exp[-t(1 - N_0)]$ [12]. The optical spectrum is the power spectrum of (5):

$$|\hat{E}(\omega;t_0)/E_0|^2 = \frac{|1 - e^{(-1+i\omega)t_0}|^2}{1+\omega^2} + \frac{e^{-2t_0}}{D(\omega)} - \frac{2e^{-t_0}}{(1+\omega^2)D(\omega)} \times \{[(1-N_0) + \omega(\omega - \Omega)](e^{-t_0} - \cos\omega t_0) - (\Omega - N_0\omega)\sin\omega t_0\}, \quad (6)$$

where $D(\omega) = (1 - N_0)^2 + (\omega - \Omega)^2$. The first term of Eq. (6) is related to the linear resonance. The second term is related to the nonlinear resonance, centered at $\omega = \Omega$, and its linewidth is narrowed by a factor $1 - N_0$. The third term of Eq. (6) is the (spectral) interference between the linear and nonlinear parts of the Fourier transform, giving "type 1" oscillating components of frequency t_0, and spectral period $\delta\nu_{T1} = t_0^{-1}$. Spectra for $N_0 = 0.3$ and 0.6 with different t_0 using Eq. (6) are shown in Fig. 3(a). We point out that these oscillations lead to an *in situ* measurement of the pump and probe delay.

We now focus on the origin of "type 2" oscillations. These take place for $N_0 \gtrsim 0.6$, where the adiabatic approximation is no longer valid. We will first analyze the case $t_0 = 0$, for which the Fourier transform of the field, $\hat{E}(\omega;0) = \int_0^\infty E_0 e^{-(pt^2+2qt)}dt$, gives

$$\hat{E}(\omega;0) = \frac{E_0}{2}\sqrt{\frac{\pi}{p}}e^{q^2/p}\,\mathrm{erfc}\,(q/\sqrt{p}), \quad (7)$$

where $p \equiv \gamma N_0(1 - i\alpha)/2$, $q \equiv [1 - N_0 + i(\Omega - \omega)]/2$, and erfc is the (complex) complementary error function. In the inset of Fig. 3(c) we represent $|\hat{E}(\omega;0)|^2$ as a function of ω. Fast oscillations are observed at the red side of the spectrum: we identify them as "type 2" oscillations. It is possible to trace back their origin from Eq. (7). The square modulus of the error function has the following dominant oscillating term: $-\cos[f(\omega)]$, $f(\omega) = [(1 - N_0)^2 - (\Omega - \omega)^2]/(2\Omega\gamma)$; the dependency on the square frequency corresponds to that observed in the experimental results [see inset of Fig. 2(c)]. The maxima are given by $f(\omega_m) = (2m + 1)\pi$, and the first one, ω_0, indicates the position of the main spectral peak. The spectral period between the first two secondary maxima ($m = 1$ and 2) gives $\delta\nu_{T2} \approx 0.2\sqrt{\alpha N_0\gamma}$. The physical origin of the type 2 oscillations is thus elucidated: it results from the strong asymmetry of the output field originated from the kicklike stimulus followed by the slow relaxation, together with the frequency chirp due to spontaneous recombination during the cavity field decay. The chirp becomes significant when the system is pumped close to the laser threshold, where the output pulse gets longer. Information on the carriers dynamics (γ) can

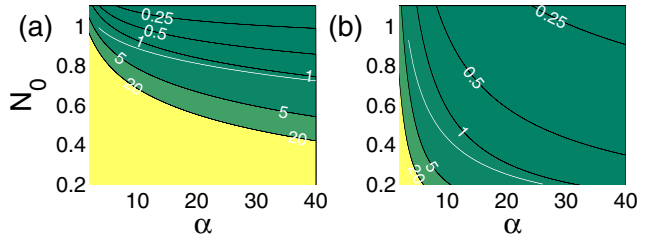

FIG. 4 (color online). Parameters map for (a) $\gamma = 0.02$ and (b) $\gamma = 1$, showing regions where type 2 oscillations are visible (dark regions), and those where they disappear (light regions). Dark lines correspond to contour plots of r defined in the text. White line is $\phi^{(2)} = \pi$ ($\delta t_E = t_a$); well below this line means $\phi^{(2)} \ll \pi$, then the adiabatic approximation becomes valid.

readily be obtained from the spectral period, and gives $\gamma \approx 0.02$, which yields $\tau_r \approx 240$ ps. This is comparable to previous measurements varying pump and probe delay [7].

For arbitrary t_0, the electric field is given by Eqs. (5), (3), and (4). Spectra for different t_0 and $N_0 = 0.9$ are represented in Fig. 3(c). The agreement with the experimental results is remarkable. Slight differences, for example, in the amplitude of type 2 oscillations, might be reduced by taking into account further effects, such as the dependence of τ_r and α on carrier density.

A criterion for the presence of "type 2" oscillations is $r \equiv |\mathrm{erf}(p_1/\sqrt{q}) - \mathrm{erf}[\mathrm{Re}(p_1/\sqrt{q})]| \sim 1$, where $(p_1, q_1) = (p, q)|_{\omega_1}$. If $r \gg 1$ or $r \ll 1$ then no oscillations are present in the power spectra. In Fig. 4 we show a two-dimensional plot of the isolines of r. Oscillations are visible in dark regions, while in light regions no oscillations are observed since $r > 20$. The minimum value for r is $r \sim 0.25$ on the top of the figure, meaning that the limit $r \ll 1$ is never reached: the oscillations only disappear through the $r \gg 1$ side. In other words, oscillations are always visible close to laser threshold. This is consistent with the experimental observations. In addition, we find that the isoline $r = 1$ is very close to the adiabatic limit $t_a = \delta t_E$ [see white line in Fig. 4(a)]. In consequence, the nonadiabatic dynamics is a necessary and sufficient condition for the occurrence of oscillations. In Fig. 4(b) we show the region of type 2 oscillations for $\gamma = 1$, which is an extrapolation for extremely high-Q systems; the nonadiabatic regime clearly spreads all over the parameter space, thus becoming ubiquitous.

In conclusion, femtosecond pump and probe of a semiconductor 2DPC for $|\Delta t| \lesssim \tau_p$ gives a handle to the amplitude and phase field dynamics. The richness of the spectral response obtained under such conditions is well captured by a simple mean field dynamical model of the nonlinear resonator. The phase modulation is translated into spectral oscillations allowing a direct access to several important parameters (α, τ_r, t_0). Let us stress that fast (type 2) oscillations are the signature of nonadiabatic dynamics, and result from a combination of both the asymmetric character of the field which develops inside the cavity after a short-pulse injection, and the frequency chirp due to carriers dynamics.

The concepts developed here constitute a framework to study field and carrier dynamics beyond the adiabatic limit. They are applicable to all active resonators provided that their normalized parameters (time-scales ratio, pumping rate, and chirp factor) fall into the parameter region presented here. Importantly, in the microscale, semiconductor PCs inherently exhibit nonadiabatic dynamics due to the closeness of the field and material relaxation time constants, a natural trend in the world of high-Q active microresonators that should be taken into account for future applications. In particular, in the context of slow light [3] and chirp management, nonadiabatic dynamics might be used to design or compensate frequency chirps originating from the interaction of short pulses with active high-Q optical resonances.

We thank C. Seassal and P. Viktorovitch for providing the sample, and N. Belabas for useful comments.

*Electronic address: Alejandro.Giacomotti@lpn.cnrs.fr

[1] The largest Q factors reported so far are of the order of 10^5; see B. S. Song *et al.*, Nat. Mater. **4**, 207 (2005).
[2] M. Soljacic and J. D. Joannopoulos, Nat. Mater. **3**, 211 (2004).
[3] M. F. Yanik and S. Fan, Phys. Rev. Lett. **92**, 083901 (2004).
[4] P. Michler *et al.*, Science **290**, 2282 (2000); S. Laurent *et al.*, Appl. Phys. Lett. **87**, 163107 (2005).
[5] For switching applications see, for example, T. Asano *et al.*, Electron. Lett. **41**, 37 (2005); T. Baba *et al.*, Electron. Lett. **39**, 1516 (2003); S. W. Leonard *et al.*, Phys. Rev. B **66**, 161102(R) (2002).
[6] For microlasers see, for example, O. Painter *et al.*, Science **284**, 1819 (1999); F. Raineri *et al.*, Appl. Phys. Lett. **86**, 011116 (2005).
[7] F. Raineri *et al.*, Appl. Phys. Lett. **85**, 1880 (2004).
[8] F. Raineri *et al.*, Opt. Lett. **30**, 64 (2005).
[9] We point out that the band diagram has two degenerated modes at the Γ point at 1540 nm [8]. We do not have any experimental evidence that the second mode couples to the incident wave. However, two-mode operation, if any, would lead to a beating in the temporal rather than in the spectral domain, which we address here.
[10] See, e.g., L. Spinelli *et al.*, Phys. Rev. A **58**, 2542 (1998).
[11] In the terminology of semiconductor lasers, α is known as the *linewidth enhancement factor*, which is usually evaluated close to the maximum of gain; in our case, the photonic mode is largely detuned with respect to the semiconductor band gap (about 90 nm), then α is strongly affected by such detuning. In our calculations we use α obtained from the experimental results as the slope of the normalized nonlinear frequency shift with respect to N_0, which gives $\alpha = 26.6$.
[12] The adiabatic regime implies exponential decay of the field if $t_a \leq (1 - N_0)/N_0\gamma$, which is verified for all α.